engineering proceedings

Proceedings

Comparing Landsat-8 OLI, Sentinel-2 MSI, and PlanetScope Imagery for Coastline Change Detection: A Case Study of El-Alamein Coast, Egypt †

Kamal Darwish [1],* and Scot Smith [2]

[1] Department of Geography, Minia University, El Minia 61519, Egypt
[2] School of Forest, Fisheries, & Geomatics Sciences, University of Florida, Gainesville, FL 32611, USA; sesmith@ufl.edu
* Correspondence: kamal.srogy@mu.edu.eg; Tel.: +2-01093566658

† Presented at the 8th International Electronic Conference on Sensors and Applications, 1–15 November 2021; Available online: https://ecsa-8.sciforum.net.

Abstract: The aim of this study is an assessment of coastline extraction and change analysis using different sensors form different satellites over-time. Three optical satellite remote sensing imageries from Landsat-8 OLI (30 m), Sentinel-2A MSI (10 m), and PlanetScope 3B (3 m) were used to detect changes of El-Alamein coastline along the Egyptian Mediterranean coast from August 2016 to August 2021. The Normalized Difference Water Index (NDWI) was applied to automate, detect and mapping water bodies based-on thresholding technique and coastline extraction. The extracted coastlines have been analyzed using Geographic Information Systems based Digital Shoreline Analysis System (DSAS.v5) model, a GIS Software tool for estimation of shoreline change rates calculated through two statistical techniques such as: Net Shoreline Movement (NSM), and End Point Rate (EPR). The results indicate differences in shoreline change rates based on different spatial resolution imageries for the same time and space.

Keywords: coastline detection; Landsat-8; Sentienal-2; PlanetScope; Alamein Coast; remote sensing; DSAS; GIS

Citation: Darwish, K.; Smith, S. Comparing Landsat-8 OLI, Sentinel-2 MSI, and PlanetScope Imagery for Coastline Change Detection: A Case Study of El-Alamein Coast, Egypt. *Eng. Proc.* **2021**, *3*, x. https://doi.org/10.3390/xxxxx

Academic Editor: Kamal Darwish

Published: 1 November 2021

1. Introduction

The coastline is the tangent line of sea and land; it is one of the most significant and morphodynamics landform in earth surface and it is prone to change in a very short period [1]. Coastline changes consider one of the major environment problems affecting the coastal zones in the world. Studies of coastline change is very important for coastal planning and management. In fact, about 80% of the world's coasts are changing with rates from 1 cm/year to 10 m/year [2]. Coastline changes under the influence of natural and anthropogenic factors [3].

Recently, satellite remote sensing techniques have become essentially for monitoring coastal change due to their large coverage, frequency and low cost [4]. A different type of images can be obtained from satellite remote sensing; Hyperspectral, Multispectral, and SAR imagery. In this study, multispectral satellite imagery were used detect coastline changes because it has several advantages, such as; a large number of data records, frequency at different times, and extensive covering of the entire planet earth [3]. The availability of time-series of optical remote sensing images can be used effectively for water bodies monitoring, coastline extraction for change analysis over-time to help understand the influence of the natural factors and human activities in coasts [5].

Water body mapping methods using spectral indices were used globally for coastline detection and extraction from Landsat satellite images because of their availability, reliability, and low cost [6]. In 2013, Landsat 8 was launched, and its Operational Land Imager

(OLI) sensor giving a multispectral images (11 spectral bands) at (30 m spatial resolution) and (16 days temporal resolution. Sentinel-2A was launched in June 2015, with identical Multispectral Instruments (MSI) capable of acquiring data in 13 bands at different spatial resolutions (between 10 m and 60 m) and 5-dayes temporal resolution at the equator [7]. Landsat-8, and Sentinel-2A giving a reliable results for water bodies mapping and change monitoring [8,9].

Planet operates PlanetScope, RapidEye and SkySat release processed data in a variety of formats to serve different uses [10]. Imagery has (4-bands) captured as a single red-green-blue (RGB) scene or. PlanetScope satellite is a CubeSat 3U form factor (10 × 10 × 30 cm). Approximately 130 satellites able to image the entire land/water surface of the Earth every day. Planet offers three levels for PlanetScope imagery: A basic scene product (level 1B), an ortho scene product (level 3B) and an ortho-tile product (level 3A) [11]. The Orth rectified surface reflectance PlanetScope-3B data has become very important for many environmental applications.

Recently, the extraction of water bodies and coastline change detection have been introduced by many researchers worldwide used Landsat time-series [3,6,12,13], sentienal2 [14], and PlanetScope imagery [15,16]. Studies Comparison of Landsat-8, sentienal-2, and PlanetScope imagery for coastline changes [17], water quality assessment [18], bathymetry mapping [17], and other combined use [19]. Previous studies assessed the shoreline morphodynamics study area using remote sensing started by Frihy and Deabes [20] used Landsat imagery from 1988 to 2011 for assessing shoreline changes. Studies of Emam and Soliman [21,22] analysed shoreline changes along Marina El-Alamein Resort based on Landsat time series TM, ETM+, and OLI between 1987 and 2017. Awad and El-Sayed [23] analysed historical changes of El-Omayed coast from 1984 to 2018 using Landsat imagery and predicate shoreline change in the future up to 2030 and 2050.

The main objective of this study is to compare the extracted coastlines from different satellites and sensors such as; Landsat-8, Sentienal-2, and PlanetScope imagery in the same time. Spatial computation of coastline change rate done using Geographic information systems and digital shoreline analysis system (DSAS) to assess accuracy of the extracted coastline and change rates along El-Alamein coast, Mediterranean Sea.

2. Materials and Methods

2.1. Study Area

The study area is located along the Mediterranean coast of Egypt. It is about 94 km west of Alexandria city and 300 km in the northwest of Cairo (Figure 1).

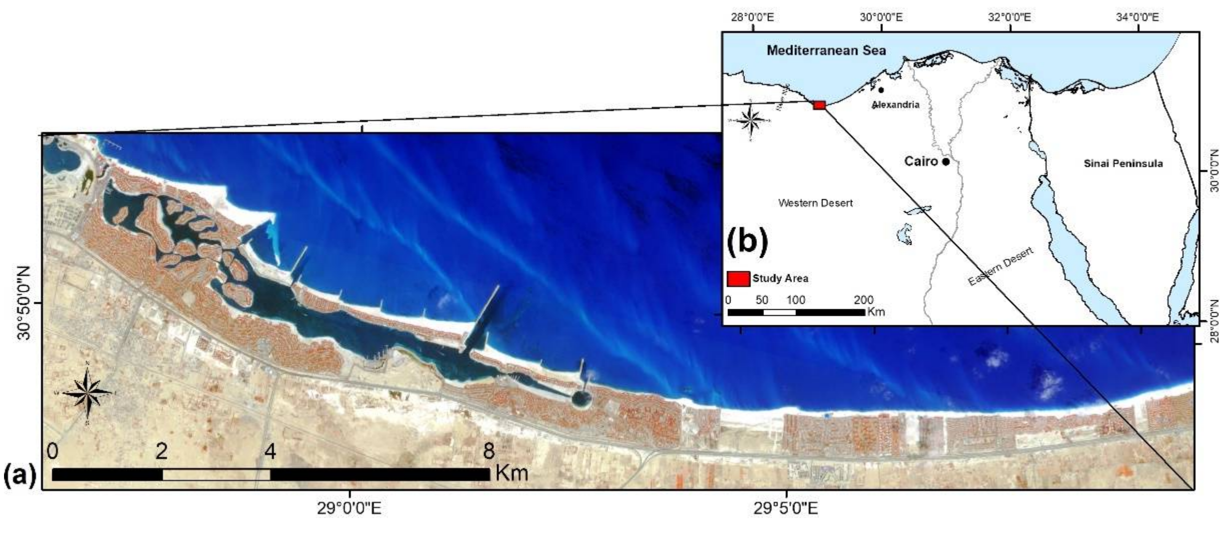

Figure 1. Location Map of the study area. Sub-figure (**a**) shows the extension of study area as appears from PlanetScope 2021 imagery, and Sub-figure (**b**) shows the location of the study area within Egypt.

2.2. Materials

Landsat-8 Operational Land Imager (OLI) images acquired in August from 2016 to 2021 with an interval (5-years) were downloaded in the GeoTIFF format from the United States Geological Survey (USGS) Earth Explorer Website (http://earthexplorer.usgs.gov/) as shown in Table 1. These Landsat datasets constitute the useable database of good Quality (level 2 product), radiometrically corrected to Surface Reflectance, free of clouds. Sentinel-2 Multispectral Instrument (MSI) Level-1C images acquired in August from 2016 to 2021 were download from the European Space Agency website. Sentinel-2A are Top of atmosphere (TOA) reflectance. PlanetScope (3 m) images acquired in August from 2016 to 2021 were collected for study area, as shown in Figure 1. The images were atmospherically corrected to surface reflectance using the 6SV2.1 radiative transfer code. The PlanetScope Lab also did radiometric correction using sensor telemetry and sensor model [18].

Table 1. Specifications of Satellite imagery used in this study.

Date	Acquired Date	Satellite/Sensor	Path/Row	Pixel Size (m)
	08/25/2016	Landsat-8/OLI	178/39	30
2016	08/20/2016	Sentienal-2A/MSI	L1C_T35RPQ	10
	08/12/2016	PlanetScope/3B	075305	3
	08/07/2021	Landsat-8/OLI	178/39	30
2021	08/14/2021	Sentienal-2A/MSI	L1C_T35RPQ	10
	08/28/2021	PlanetScope/3B	082015	3

[1] Landsat downloaded from USGS Website: https://earthexplorer.usgs.gov/, Sentienal-2A downloaded from https://scihub.copernicus.eu/dhus/#/home, PlanetScope downloaded from https://www.planet.com.

2.3. Methods

The methods of this study are divided into three stages; (1) remote sensing data collection and preprocessing such as band combination, geometrical and radiometric corrections. (2) Applied NDWI/MNDWI indices for automatic coastline extraction. Moreover (3) GIS based spatial analysis of coastline changes using Digital Shoreline Analysis System (DSAS) is a GIS-based system established by the USGS. Publicly available, at http://woodshole.er.usgs.gov/project-ages/dsas/. DSAS calculates gaps amongst the coastline positions during defined periods as shown in Figure 3. Normalized Difference Water Index (NDWI)/Modified Normalized Difference Water Index (MNDWI) water indices applied for study area using ERDAS Imagine 2015 algorithms to detect the water/land feature by thresholding method using ENVI 5.3 software for coastline detection as shown in Figure 2. NDWI was proposed by McFeeters (1996) for water resource assessment. An NIR band and a green band are used to enhance the discrepancies between surface water and non-water features [24]. McFeeters's NDWI is calculated in Equation (1) as:

$$\mathbf{NDWI} = \frac{(\mathbf{Band}_{\mathbf{Green}} - \mathbf{Band}_{\mathbf{NIR}})}{(\mathbf{Band}_{\mathbf{Green}} + \mathbf{Band}_{\mathbf{NIR}})} \tag{1}$$

where $\mathbf{Band}_{\mathbf{Green}}$ is the reflectance value of the green band and $\mathbf{Band}_{\mathbf{NIR}}$ reflection value of the NIR band. The derived new index is called MNDWI [25], which is expressed in Equation (2) as:

$$\mathbf{MNDWI} = \frac{\mathbf{Band}_{\mathbf{Green}} - \mathbf{Band}_{\mathbf{MIR}}}{\mathbf{Band}_{\mathbf{Green}} + \mathbf{Band}_{\mathbf{MIR}}} \tag{2}$$

where $\mathbf{Band}_{\mathbf{MIR}}$ is the reflectance of the MIR band. The index NDWI were applied on PlanetScope imagery (4 bands), while Landsat-8 and Senttienal-2A applied MNDWI.

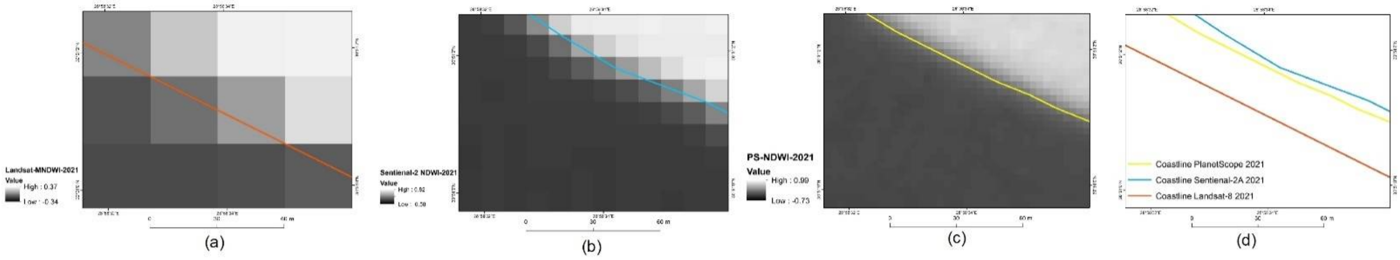

Figure 2. Coastline feature extraction. Sub-figure (**a**) Coastline extraction from Landsat-8 MNDWI August 2021, sub-figure (**b**) coastline extraction from Sentienal-2A NDWI August 2021, (**c**) coastline extraction from PlanetScope NDWI August 2021, and subfigure (**d**) spatial displacement between coastlines at the same time August 2021.

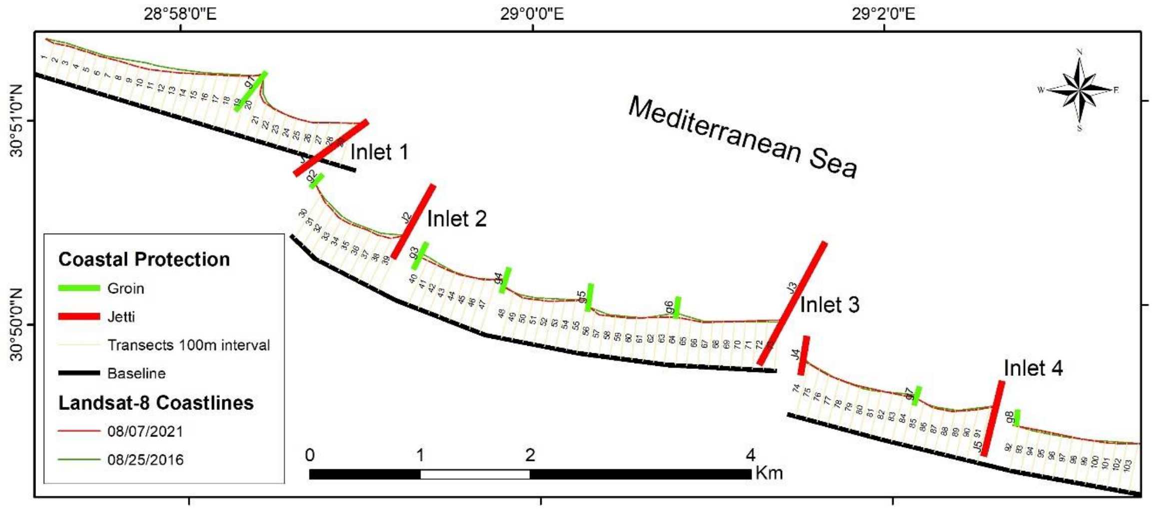

Figure 3. Show the coastline change analysis method using DSAS**.**

3. Results

Analysis of coastline changes from three different satellites with different spatial resolution for the same time-period from august 2016 to august 2021 indicated that there is difference in Net Shoreline Movement and End Point Rate there along 100 transects with 100-m spatial interval as shown in Figure 4. Summarized results of shoreline change rates statistics and Net Shoreline Movement are shown in Table 2. In addition, there is a difference of the highest accretion distance between Landsat-8 and Sentienal-2 reach (10 m) and between Landsat-8 and PlanetScope is (6 m). The highest annual rate of coastal erosion and accretion in study area is nearly close to ±2 m/y.

Table 2. Statistics of coastline change difference between 2016 to 2021.

Parameter			Landsat-8	Sentienal-2	PlanetScope
NSM [1]		Highest Accretion	49.83	39.87	43.84
		Highest Erosion	−15.97	−22.44	−18.61
		Highest	−3.23	−4.6	−3.69
	Erosion	Average	−1.50	−1.48	−0.02
		Lowest	−0.11	−0.01	−1.19
EPR [2]		Highest	10.07	8.0	8.70
	Accretion	Average	3.06	1.50	1.52
		Lowest	0	0	0.01

[1] Net Shoreline Movement (m), [2] End Point Rate(m/y).

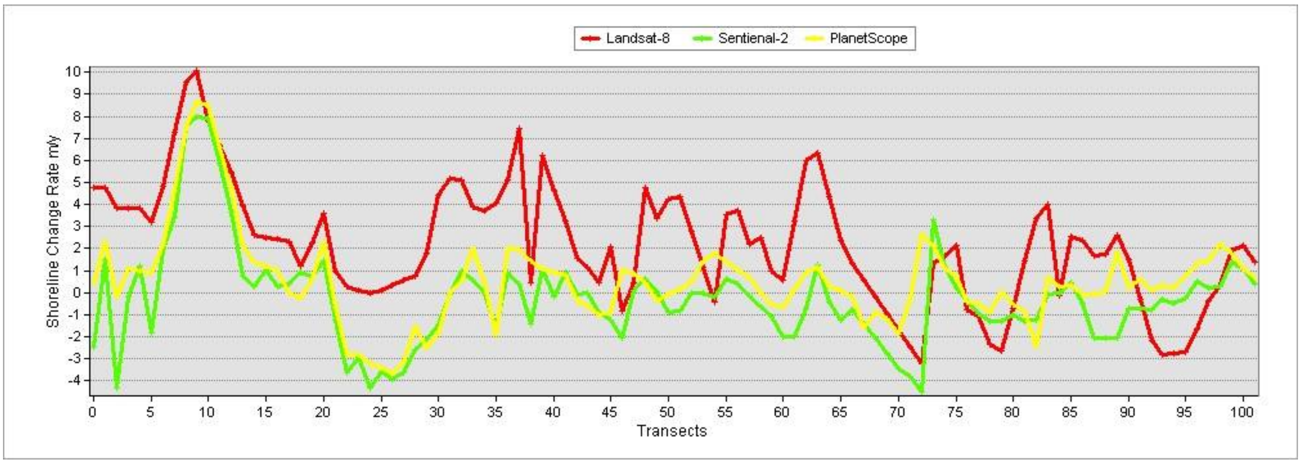

Figure 4. Comparing coastline change rates using different satellite data between 2016 and 2021.

Spatial variations of shoreline change rate over study area refers to an difference of medium and high spatial resolution of satellite data, in the first transects (1–6) landsat-8 data give an accretion rates about 3 m/y; while Sentinel Data give Negative values reach to 4 m/y. In addition, a big difference in coastline change rates appear in the transects (20–30), the shoreline which come from landsat-8 are higher the negative values from Sentienal-2 data. While, the last transects between (90–100) shoreline rates from landsat-8 is lower than PlanetScope and Sentienal-2 rates. The results from this study indicated that the rates came from sentienal-2 is closely to rates of PlanetScope imagery than landsat-8 rates as shown in Figures 3 and 4.

4. Discussion

The analysis of the extracted shorelines from different remote sensing satellite data shows that a difference in shoreline change rate. It clear the water bodies and coastline extraction more accurately and clean from the high-resolution PlanetScope imageries (3 m) and Sentienal-2A (10 m) than Landsat-8 (30 m). The accurately of coastline effect on the change detection maps and rate-of change. Study area has facing dramatically shoreline morphodynamics and it is protected by 8-short groins and 5-Jetties to protected the coastline and four artificial inlets. Coastline detection for this study area is very important because recent urban planning and resorts. Figure 5, shows the correlation between the shoreline change rates from Landsat, Sentienal2, and PlanetScope. It is clear that there is a strong linear relationship between PlanetScope and Sentienal-2 rates, on the other hand Landsat-8 give weak correlation between Landsat and PlanetScope and Sentienal-2 Rates.

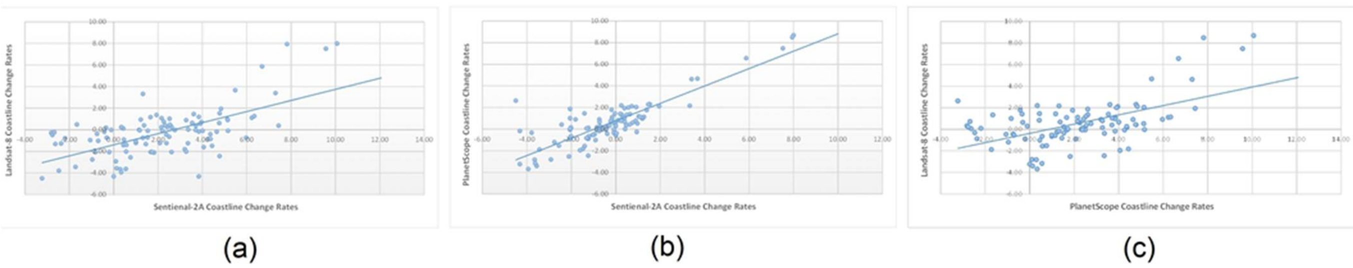

Figure 5. Correlation and linear relationship between different coastline rates. (**a**) The correlation between Landsat-8 and Sentienal-2 shoreline change rates, (**b**) the correlation between PlanetScope and Sentienal-2 shoreline change, and subfigure(**c**) the correlation between Landsat-8 and PlanetScope shoreline change.

5. Conclusions

This work is the first study comparing three different satellite data from medium to high-resolution imagery to detect and extract linear coastline features as well as change analysis. All of satellite images used in this study are valid for coastline change detection with a percent of accuracy. It is cleared that coastline features is more reliable and strong correlation from the high-spatial resolution imagery (PlanetScope), and (Sentienal-2A) than Landsat imagery. Landsat-8 imagery give a higher rate of change from PlanetScope and Sentienal-2A imagery for the same time. PlanetScope giving very accurate shoreline—positions and protection features than Landsat-8 and Sentienal-2A imagery. It is strongly recommended to use a high spatial resolution (PlanetScope) to higher accurately coastline change detection.

Author Contributions: Both authors contributed to all parts equally. Both authors have read and agreed to the published version of the manuscript.

Funding: This work has not been supported by any institutions.

Institutional Review Board Statement:

Informed Consent Statement:

Data Availability Statement:

Conflicts of Interest: The authors declare no conflict of interest.

References

1. Yasir, M.; Sheng, H.; Fan, H.; Nazir, S.; Niang, A.J.; Salauddin, M.D.; Khan, S. Automatic Coastline Extraction and Changes Analysis Using Remote Sensing and GIS Technology. *IEEE Access* **2020**, *8*, 180156–180170, doi:10.1109/ACCESS.2020.3027881.
2. Kermani, S.; Boutiba, M.; Guendouz, M.; Guettouche, M.S.; Khelfani, D. Detection and analysis of shoreline changes using geospatial tools and automatic computation: Case of jijelian sandy coast (East Algeria). *Ocean Coast. Manag.* **2016**, *132*, 46–58.
3. Pardo-Pascual, J.E.; Almonacid-Caballer, J.; Ruiz, L.A.; Palomar-Vázquez, J. Automatic extraction of shorelines from Landsat TM and ETM+ multi-temporal images with subpixel precision. *Remote Sens. Environ* **2012**, *123*, 1–11.
4. Boak, E.H.; Turner, I.L. Shoreline Definition and Detection: A Review. *J. Coast. Res.* **2005**, *21*, 688–703.
5. Olmanson, L.; Brezonik, P.; Bauer, M. Remote Sensing for Regional Lake Water Quality Assessment: Capabilities and Limitations of Current and Upcoming Satellite Systems. In *The Handbook of Environmental Chemistry*; Springer: Cham, Switzerland, 2015; Volume 33, pp. 111–140.
6. Milad, N.-J.; Bovolo, F.; Bruzzone, L.; Gege, P. Physics-based Bathymetry and Water Quality Retrieval Using PlanetScope Imagery: Impacts of 2020 COVID-19 Lockdown and 2019 Extreme Flood in the Venice Lagoon. *Remote Sens.* **2020**, *12*, 2381.
7. Cui, B.; Li, X. Coastline change of the Yellow River estuary and its response to the sediment and runoff (1976–2005). *Geomorphology* **2011**, *127*, 32–40.
8. Nguyen, U.N.T.; Pham, L.T.H.; Dang, T.D. An automatic water detection approach using Landsat 8 OLI and Google Earth Engine cloud computing to map lakes and reservoirs in New Zealand. *Environ. Monit. Assess.* **2019**, *191*, 235.
9. Ansper, A.; Alikas, K. Retrieval of Chlorophyll a from Sentinel-2 MSI Data for the European UnionWater Framework Directive Reporting Purposes. *Remote Sens.* **2019**, *11*, 64.
10. Planet. Planet Imagery Product Specification. 2021. Available online: https://assets.planet.com/docs/ Combined-Imagery-Product-Spec-Dec-2018.pdf (accessed on 28 September 2021).
11. Gabr, B.; Ahmed, M.; Marmoush, Y. PlanetScope and Landsat 8 Imageries for Bathymetry Mapping. *J. Mar. Sci. Eng.* **2020**, *8*, 143.
12. Dewi, R.S.; Bijker, W. Dynamics of shoreline changes in the coastal region of Sayung, Indonesia. *Egypt. J. Remote Sens. Space Sci.* **2020**, *23*, 181–193. https://doi.org/10.1016/j.ejrs.2019.09.001.
13. Darwish, K.; Smith, S.E.; Torab, M.; Monsef, H.; Hussein, O. Geomorphological changes along the Nile Delta coastline between 1945 and 2015 detected using satellite remote sensing and GIS. *J. Coast. Res.* **2017**, *33*, 786–794. https://doi.org/10.2112/JCOASTRES-D-16-00056.1.
14. Astiti, S.; Osawa, T.; Nuarsa, I. Identification Of Shoreline Changes Using Sentinel 2 Imagery Data In Canggu Coastal Area. *ECOTROPHIC J. Environ. Sci.* **2019**, *13*, 191–204. https://doi:10.24843/EJES.2019.v13.i02.p07.
15. Kelly, J.T.; Gontz, A.M. Rapid assessment of shoreline changes induced by Tropical Cyclone Oma using CubeSat imagery in southeast Queensland, Australia. *Journal of Coastal Research* **2020**, *36*, 72–87. Coconut Creek (Florida), ISSN 0749-0208.
16. Park, S.J.; Achmad, A.R.; Syifa, M.; Lee, C.-W. Machine learning application for coastal area change detection in Gangwon province, South Korea using high-resolution satellite imagery. *J. Coast. Res.* **2019**, *90*, 228–235.
17. Mitri, G.; Nader, M.; Abou Dagher, M.; Gebrael, K. Investigating the performance of sentinel-2A and Landsat 8 imagery in mapping shoreline changes. *J Coast Conserv* **2020**, *24*, 40. https://doi.org/10.1007/s11852-020-00758-4.
18. Mansaray, A.S.; Dzialowski, A.R.; Martin, M.E.; Wagner, K.L.; Gholizadeh, H.; Stoodley, S.H. Comparing PlanetScope to Landsat-8 and Sentinel-2 for Sensing Water Quality in Reservoirs in Agricultural Watersheds. *Remote Sens.* **2021**, *13*, 1847. https://doi.org/10.3390/rs13091847.

19. Mandanici, E.; Bitelli, G. Preliminary Comparison of Sentinel-2 and Landsat 8 Imagery for a Combined Use. *Remote Sens*. **2016**, *8*, 1014. https://doi.org/10.3390/rs8121014.
20. Frihy, O.; Deabes, E. Erosion chain reaction at El-Alamein Resorts on the western Mediterranean coast of Egypt. *Coast Eng*. **2012**, *69*, 12–18.
21. Emam, W.W.M.; Soliman, K.M. Applying geospatial technology in quantifying spatiotemporal shoreline dynamics along Marina El-Alamein Resort, Egypt. *Environ. Monit. Assess.* **2020**, *192*, 459. https://doi.org/10.1007/s10661-020-08432-w.
22. Emam, W.W.M.; Soliman, K.M. Quantitative analysis of shoreline dynamics along the Mediterranean coastal strip of Egypt. Case study: Marina El-Alamein resort. In *Environmental remote sensing in Egypt*; Elbeih, S., Negm, A., Kostianoy, A., Eds.; Springer: Cham: Switzerland, 2020.
23. Awad, M.; El-Sayed, H.M. The analysis of shoreline change dynamics and future predictions using automated spatial techniques: Case of El-Omayed on the Mediterranean coast of Egypt. *Ocean Coast. Manag.* **2021**, *205*, 105568 https://doi.org/10.1016/j.ocecoaman.2021.105568.
24. McFeeters, S.K. The use of the Normalized Difference Water Index (NDWI) in the delineation of open water features. *Int. J. Remote Sens.* **1996**, *17*, 1425.
25. Xu, H. Modification of normalised difference water index (NDWI) to enhance open water features in remotely sensed imagery. *Int. J. Remote Sens.* **2006**, *27*, 3025–3033.